Primary photophysics of the FMN binding LOV2 domain of the plant blue light receptor phototropin of Avena sativa

ARTICLE *in* CHEMICAL PHYSICS · NOVEMBER 2003

Impact Factor: 1.65 · DOI: 10.1016/S0301-0104(03)00390-2

Available online at www.sciencedirect.com
SCIENCE DIRECT®
Chemical Physics 294 (2003) 501–508
Chemical Physics
www.elsevier.com/locate/chemphys

Primary photophysics of the FMN binding LOV2 domain of the plant blue light receptor phototropin of *Avena sativa*

Tanja A. Schüttrigkeit [a], Christian K. Kompa [a], Michael Salomon [b,1], Wolfhart Rüdiger [b], Maria E. Michel-Beyerle [a,*]

[a] *Institut für Physikalische und Theoretische Chemie, Technische Universität München, Lichtenbergstr. 4, 85747 Garching, Germany*
[b] *Botanisches Institut der Universität München, Menzinger Strasse 67, München 80638, Germany*

Received 21 July 2003

Abstract

The temporal evolution of the initially excited singlet state of flavine mononucleotide, which is the cofactor in the LOV2 domain of the blue photoreceptor phototropin, has been studied in picosecond time-resolved fluorescence and femtosecond time-resolved absorption experiments. In the LOV2-WT protein of *Avena sativa* singlet–triplet intersystem crossing proceeding within 2.3 ns is the primary process which increases the triplet yield by a factor of 1.23 as compared to a mutant where cysteine 39 is replaced by alanine. This flavin triplet state is responsible for the formation of a cysteinyl–flavin adduct which triggers the unique photocycle of the LOV2 domain and thus the sensoric function of the blue light receptor phototropin.

1. Introduction

A wide range of phenomena in the life of plants including seed germination, pigment biosynthesis, stomatal opening, floral induction, circadian rhythms, and phototropism is initiated by sensoric photoreceptors [1]. Depending on the spectral region, the photoactive cofactors may be bilins in phytochromes responding to red light [2] and flavins in the blue light photoreceptors, i.e., the recently discovered cryptochromes [3,4] and phototropins [5]. Phototropins may bind flavin mononucleotide (FMN) in two light-, oxygen-, and voltage-sensitive domains, LOV1 and LOV2 with a molecular weight of 12.1 kDa. Their absorption and fluorescence excitation spectra were found to be similar and to resemble closely the action spectrum of phototropin [6].

The fingerprint for the sensoric function in this class of blue photoreceptors is the dramatic bleaching under high excitation intensity. Comparison of the absorption spectra of the LOV domains under bleaching conditions and of mercuric ion reductase [7] led to the conclusion that the transient product state with an absorption maximum at 390 nm is a flavin carbon C(4a)–thiol

* Corresponding author. Fax: 89-289-13026.
E-mail address: michel-beyerle@ch.tum.de (M.E. Michel-Beyerle).
[1] Present address: Vertis Biotechnologie A.G., Lise-Meitner-Str. 30, 85356 Freising, Germany.

0301-0104/$ - see front matter © 2003 Published by Elsevier B.V.
doi:10.1016/S0301-0104(03)00390-2

adduct. In LOV2 this metastable adduct is formed within 4 μs from an intermediate which resembles the flavin triplet state on the basis of its absorption spectrum. This adduct recovers spontaneously with a halftime of ~50 s [8]. The observation that the adduct does not form in the mutant LOV2-C39A points independently to the decisive role of cysteine at position 39 being the amino acid of central importance for the initiation of the reversible photocycle [6,8].

These conclusions on the mechanism are confirmed by the X-ray structural analysis [9] of the LOV2 domain from *Adiantum capillus-veneris* phy3 (at 2.7 Å resolution). A single molecule of FMN is bound non-covalently in the interior of the protein by a network of hydrogen bonds as well as van der Waals and electrostatic interactions. The flavin-binding pocket is primarily polar on the pyrimidine side of the isoalloxazine ring and non-polar around the dimethylbenzene moiety. There are two buried water molecules, one forming a hydrogen bond to the 2′hydroxyl group of the ribityl chain and the other to the flavin's 3′hydroxyl group; both water molecules form hydrogen bonds to the side chain of asparagine 965. Most relevant for the mechanism of adduct formation is the observation that there is no indication of a hydrogen bond to nitrogen 5 of the flavin isoalloxazine moiety. Spectroscopic investigations on LOV1-WT and LOV2-WT domains and mutants of *Avena sativa* [6] have shown that cysteine C39 is not essential for flavin binding but is crucial for the reversible photocycle depicted in Fig. 1. On the basis of dark-light difference absorption spectra [6] and NMR investigations [10] the formation of a C(4a)-cysteinyl adduct has been postulated. In fact, the more recent X-ray structural analysis of LOV2-WT (*Adiantum capillus-veneris* phy3) in its bleached state revealed a unique photochemical switch in the flavin binding pocket, where the absorption of light drives the formation of a reversible covalent bond between a well conserved cysteine residue and the flavin cofactor at the carbon atom (4a) [11]. This structural work provides a highly resolved (2.3 Å) molecular picture of a cysteinyl–flavin covalent adduct which is responsible for phototropin kinase activation and subsequent signal transduction. These studies show (i) a ~8° tilt of the FMN isoalloxazine ring and (ii) the rotation of the C39 side chain by 100° around the C_α–C_β bond which induces a displacement of the sulfur atom by 2.3 Å. This sulfur atom is now located within covalent bonding distance of the carbon (4a) of FMN.

In the past the transient triplet state which initiates the unique photocycle of the LOV2 domain has been studied on time scales longer than 30 ns [12] and more recently, while this work was in progress, with femtosecond time resolution [13]. The conclusions of these most recent investigations of LOV2-WT from *Adiantum capillus-veneris* phy3 and *Avena sativa* are based on a comparison of the primary photodynamics of LOV2-WT protein and FMN free in aqueous solution. These conclusions are only partially confirmed in the present approach which compares LOV2-WT from *Avena sativa* and the single-site mutant C39A where cysteine has been replaced by alanine.

As indicated in the kinetic scheme (Fig. 1), triplet formation may in principle proceed via two different mechanisms: singlet–triplet intersystem crossing (ISC) and singlet–triplet spin-conversion in a singlet phased primary radical pair, which is induced by hyperfine interaction [14,15]. As extensively shown in the recent literature oxidized flavin in its excited singlet state may indeed take up an electron from a nearby tyrosine or tryptophane [16,17]. In the structure of the LOV2 domain the four potential candidates with electron donor properties are the amino acid residues Y29, Y72 and Y97 and W80, which are located at average center-to-center distance from flavin of ~14 Å. In the context of this paper it should be added, that at high light intensities the photogenerated triplet state has been shown to act as a potent oxidant [18] for redox active amino acid residues in a mutant with a triplet lifetime exceeding the one of the native LOV2 domain.

2. Experimental

2.1. Cloning, site-directed mutagenesis, expression, and purification of LOV2 and LOV2-C39A

Cloning of the LOV2 domain of the cDNA from *Avena sativa* Phot1 into the bacterial

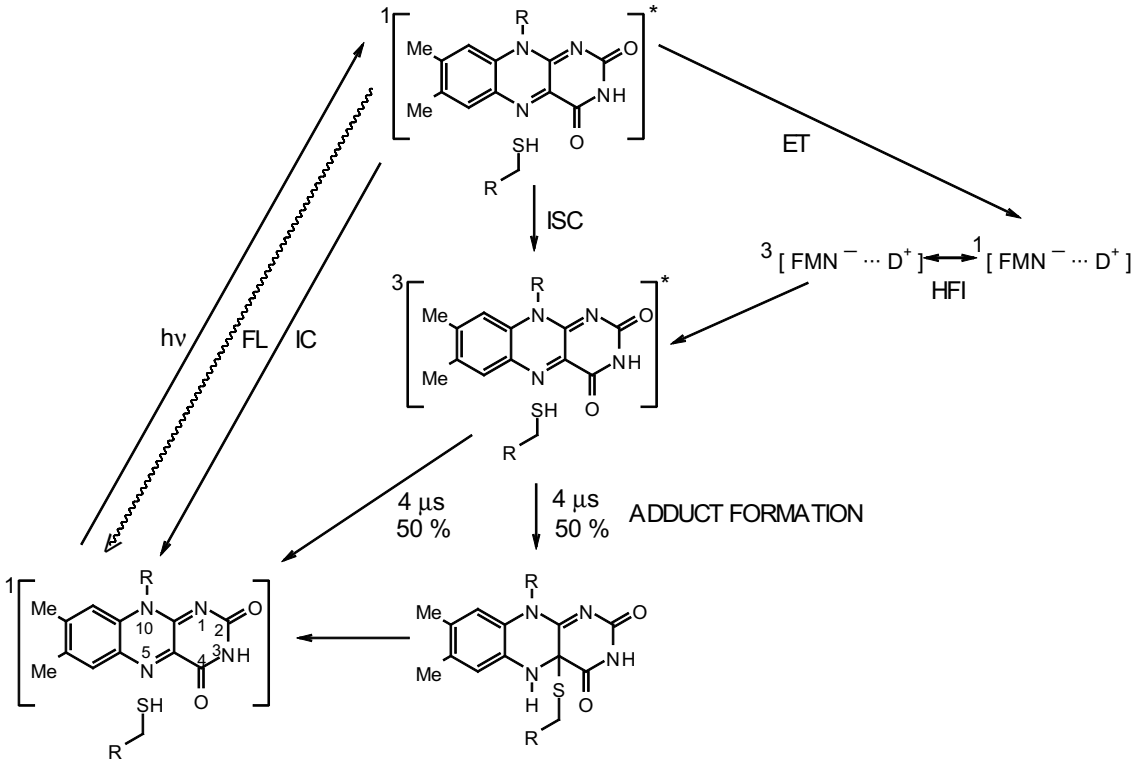

Fig. 1. Photocycle of the LOV2 domain, R-SH indicating cysteine Cys39. Potential deactivation channels of the singlet excited state ^{1}FMN* are fluorescence (FL), internal conversion (IC), formation of triplet state ^{3}FMN* via intersystem crossing (ISC) or radical pair recombination following spin conversion induced by hyperfine interaction (HFI). In the latter case the primary process is the reduction of FMN by a nearby donor species (D) which may be tryptophane or tyrosine.

expression vectors pCAL-n-EK as a fusion to the calmodulin binding peptide (CBP) was carried out as described recently [19]. The mutant C39A has been generated by site-directed mutagenesis to generation the mutant LOV2 protein LOV2-C39A was performed according to the Quick Change protocol from Stratagene. For expression of the fusion proteins the *Escherichia coli* host strain BL21(DE3) pLysS was used. Expression of the LOV proteins was induced by the addition of isopropyl β-D-galactopyranoside (1 mM, final concentration) when the culture has reached an OD_{600} of 0.2–0.3. Expression was carried out at 30 °C in the dark for 3.5 h. Cells were lysed overnight at −20 °C in the presence of 0.2% Triton-X 100. Purification of the CBP-fusion proteins on calmodulin resin was performed according to the instructions of Stratagene. The purified fusion proteins were stored at 4 °C in high-salt elution buffer (1 M NaCl, 50 mM Tris–HCl, pH 8.0, 10 mM β-mercaptoethanol, 2 mM EGTA).

2.2. Steady-state spectroscopy

Absorption spectra were recorded with an UV–VIS spectrometer (Perkin–Elmer Lamda 23) with 2.0 nm resolution. Fluorescence spectra were measured using a spectrofluorometer (Spex Fluorolog-2 Model F212I) with 1.7 nm resolution or better. A 2 mm path-length quartz cuvette was used. To perform low-temperature experiments the cuvette was placed in a continuous-flow cryostat (Leybold VSK 3–300) cooled with liquid nitrogen. For the fluorescence measurements at low excitation intensity the integration time was 0.1 s and the slits were adjusted to 0.2 mm for the excitation

beam and 1.0 mm for the detection monochromator. For the high intensity measurements the slits were opened to 2.0 mm, the integration time was 1.0 s.

2.3. Fluorescence quantum yields

For determination of the fluorescence quantum yields of LOV2-WT and LOV2-C39A, samples were diluted to an OD of 0.047. As standard a solution of fluorescein in 0.1 M NaOH was used ($\Phi_{FL} = 0.925$) [20]. All measurements were carried out in quartz cuvettes with a path length of 2 mm.

2.4. Picosecond time-resolved fluorescence measurements

Measurements were performed with an excitation wavelength of 444 nm using the frequency-doubled output of a Ti:Sapphire laser (Coherent MIRA) combined with a pulse-picker (Coherent 9200) reducing the repetition rate to 3.8 MHz. For detection of fluorescence kinetics a time-correlated single-photon counting setup (TCSPC) was used [21]. The instrument response function was 27.1 ps. All data were measured under magic angle conditions. Using standard deconvolution procedures averaged lifetimes carry an approximate error of $<20\%$.

2.5. Femtosecond transient absorption measurements

Transient absorption measurements were performed using a Ti:Sapphire oscillator/regenerative amplifier system which has been described in detail elsewhere [22]. Briefly, the output at 780 nm of an Ar^+-laser pumped commercial Ti:Sapphire oscillator (MIRA/Coherent, repetition rate 76 MHz, pulse width 100 fs) was temporarily broadened to 150 ps before seeding a regenerative amplifier system (BMI Alpha 1000S) pumped at 10 W by a Nd:YLF laser (BMI 621D) at 526 nm. The amplified pulses (1.4 mJ) were split into pump and probe beam (9:1). After separate recompression optical pulses at 780 nm with a pulse duration of 120 fs were obtained. The more intense pulses were frequency-doubled and directed through an OPG/OPA setup to produce a signal wave tunable from 450 to 700 nm for excitation. The weaker probing pulses were sent to a variable delay line four times allowing a total delay between pump and probe pulses of 10 ns with increments of 66 fs before they were focused in a 2 mm sapphire crystal to produce a white light continuum. By means of a chirp-compensated, stepper motor controlled spectrometer, a spectral region with a bandwidth of 12 nm was selected from this continuum. The relative polarization between pump and probe beam was set to the magic angle to avoid rotational depolarization effects. Pump and probe beams were focused under an angle of 8° at a 2 mm fused silica cuvette containing the sample.

3. Results and discussion

3.1. Steady-state spectroscopy

All time-resolved measurements are based on the steady-state absorption, fluorescence and fluorescence excitation spectra of the LOV2-WT domain and LOV2-C39A mutant taken at low light intensity at 298 K. Figs. 2(a) and (b) show that the respective spectra for LOV2-WT and LOV2-C39A are nearly identical.

In analogy to spectroscopic features of oxidized flavins the positions of the absorption peaks at 373 and 447 nm of both WT and mutant are assigned to the $S_0 \rightarrow S_2$ and the $S_0 \rightarrow S_1$ transitions, respectively. Considering the high sensitivity of the $S_0 \rightarrow S_2$ absorption band of oxidized flavin to the polarity of the environment [23], it is interesting to note that in both proteins the position of this band resembles the one of FMN free in aqueous solution. This similarity is consistent with the highly polar pyrimidine site of the isoalloxazine ring in the protein pocket [11]. Within the $S_0 \rightarrow S_1$ absorption band a vibronic structure is clearly resolved in the protein. This feature points to a reduction of inhomogeneous broadening of the flavin chromophore fixed in this protein binding pocket as compared with FMN in solution. Deconvolution with three Gaussian profiles results in peaks for LOV2-WT/LOV2-C39A at 425 nm/428 nm, 449 nm/450 nm and 475 nm/476 nm with an

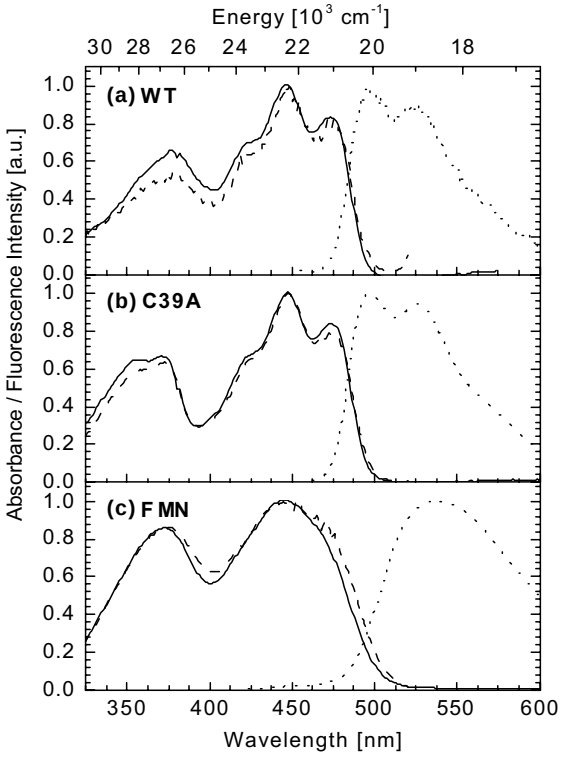

Fig. 2. Steady-state absorption (—), fluorescence (···, $\lambda_{EXC} = 475$ nm) and fluorescence excitation (- - -, $\lambda_{PROBE} = 525$ nm) spectra at 298 K and low intensity of (a) LOV2-WT, (b) LOV2-C39A, and (c) FMN free in aqueous solution at pH 8.

average full-width-half-maximum (FWHM) of 600 cm^{-1} exhibiting a relative intensity of 0.3:0.4:0.3 and a vibronic progression of approximately 1200 cm^{-1}. This progression is in agreement with previous observations on oxidized flavins in nonpolar solutions [24,25]. As to be expected, the fluorescence excitation spectrum follows the absorption spectrum.

The fluorescence spectra of both LOV2 samples show also vibrational progression responsible for two maxima which can be deconvoluted into two vibrational bands peaking at 493 and 520 nm. The vibronic progression of 1070 cm^{-1} in the ground state is slightly smaller than for the excited state. Since the relative amplitudes of these emission bands are 0.4:0.6, they are not a mirror image of the corresponding absorption spectrum. This effect has been observed previously for free flavins in frozen solution at 77 K [25] as well as for the flavin fluorescence spectrum of the LOV1 domain of *Clamydomonas reinhardtii* Phot1, WT and mutant where cysteine is replaced by serine [26]. If the lifetime of the excited electronic singlet state S_1 is sufficiently long for the excited molecules to attain thermal equilibrium, the fluorescence emission occurs primarily from the zero-point vibrational level of S_1. If the nuclear configurations of the ground and excited electronic states are sufficiently similar, the vibrational wave functions are the same. This assumption is the basis for the empirical mirror symmetry relation between the fluorescence and absorption spectra which is commonly observed in condensed media and also reported for the preparations of the LOV2 domain described in [13]. Deviations from mirror symmetry as encountered in the fluorescence spectra of the LOV2 domain in Fig. 2 as well as the LOVl protein indicate differences in the nuclear configurations in the electronic ground and excited states, S_0 and S_1.

In contrast to FMN bound to either LOV2-WT or LOV2-C39A, the spectra of free FMN in aqueous solution at pH 8.0 are devoid of vibronic structure. Nevertheless, a similar numerical analysis results in three vibronic absorption bands, peaking at 425, 447 and 471 nm. The average FWHM of these bands is 800 cm^{-1} and, therefore, larger than in LOV2 protein. The vibronic progression is 1150 cm^{-1}. The peak positions and relative amplitudes coincide with the results for the protein samples. Similarly, the fluorescence band of FMN in the protein pocket is composed of two vibronic transitions peaking at 511 nm and 541 nm (equivalent to a progression of 1100 cm^{-1}) and the relative amplitudes of these bands are 0.3 and 0.7.

The comparison of LOV2-WT, mutant C39A and free flavin shows that the Stokes shift of the protein samples ($\Delta E_{Stokes} \approx 770$ cm^{-1}) is considerably smaller than the one of FMN dissolved in aqueous solution ($\Delta E_{Stokes} \approx 1662$ cm^{-1}). This difference clearly points to the enhancement of nuclear relaxation of excited flavin and its aqueous surroundings as compared to flavin bound in the protein pocket of the LOV2 domain [27,28].

Although the main features of the steady-state spectra are the same in WT and mutant, the

fluorescence quantum yields Φ_{FL} differ for the two species: $\Phi_{FL} = 0.14$ for wildtype and $\Phi_{FL} = 0.26$ for the mutant LOV2-C39A. Since steady-state measurements cannot account for contributions of thermally activated delayed fluorescence according to $T_1 \rightarrow S_1$, these contributions can be disregarded on the basis of energetics: $\Delta E(S_1 \rightarrow T_1) \approx 0.31$ eV [29,30] assuming that the $S_1 \rightarrow T_1$ energy gap of oxidized flavin is more or less invariant for FMN in the two proteins and solution.

3.2. Time-resolved spectroscopy

The fluorescence decay of LOV2-WT and LOV2-C39A is shown in Fig. 3. Both traces can be fitted monoexponentially to a time constant of 2.2 ns for WT and 4.3 ns for the mutant. The fluorescence lifetime of the mutant is comparable to the lifetime of free FMN in aqueous solution at pH 7 which has been determined to be 4.6 ns [31].

In order to identify potential decay channels underlying the excited state lifetime, time-resolved absorption kinetics have been followed at 550 and 650 nm with 200 fs resolution (Fig. 4). Probing at 550 nm allows to follow stimulated emission ($S_1 \rightarrow S_0$) as reflected in negative sign of the difference absorbance. This signal decays monoexponentially with the time constant of the fluorescence measurements (Fig. 3).

The positive difference absorbance monitored at 650 nm which is one of the two near-IR peak positions of the triplet absorption spectrum grows

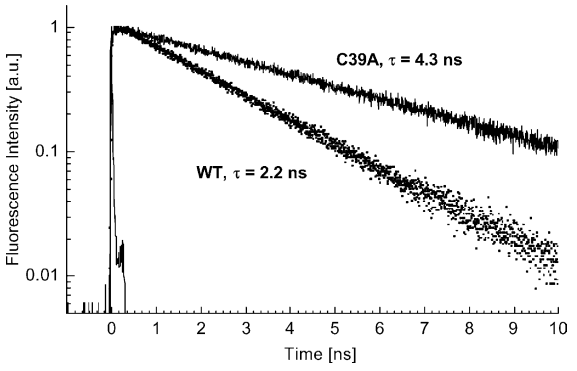

Fig. 3. Fluorescence decay pattern of LOV2-WT and LOV2-C39A at 298 K ($\lambda_{EXC} = 443$ nm, $\lambda_{PROBE} = 495$ nm). Instrument response function 27 ps.

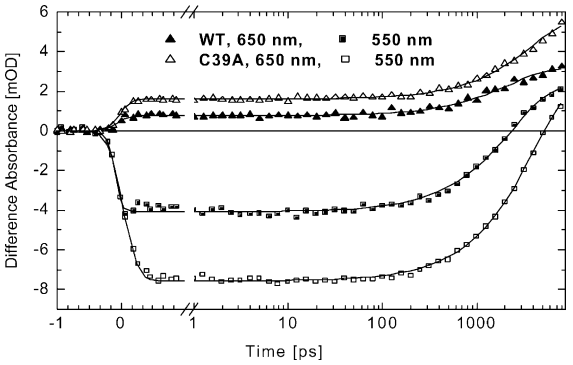

Fig. 4. Evolution of stimulated emission probed at 550 nm and triplet absorption probed at 650 nm of LOV2-WT and LOV2-C39A. Time resolution 200 fs.

in with the time constant of the decay of both, stimulated emission and fluorescence. At times <100 ps the signal reflects the excited state absorption $S_1 \rightarrow S_n$, whereas due to its larger extinction coefficient at longer times the triplet absorption predominates. The formation of a radical pair involving the FMN semiquinone neutral radical or radical cation can be excluded on the basis of the absorption spectra of these species [8,32]. The positive difference absorption emerging at 550 nm is indicative of increasing triplet state absorption also at this wavelength [33]. In summary the temporal traces in Figs. 3 and 4 do not show any intermediate states different from the triplet state. Thus these results exclude deactivation processes like internal conversion and charge separation on the sub-ns time scale. They exclude also triplet formation via recombination of a primary radical pair after hyperfine induced $S_1 \rightarrow T_1$ conversion on the ns-time scale.

Information on the relative efficiency of $S_1 \rightarrow T_1$ ISC is given by the ratio of the absorption signal at long delay times representing the $T_1 \rightarrow T_n$ transition and the initial signals related to the excited singlet state, i.e., the $S_1 \rightarrow S_n$ transition probed at 650 nm and the $S_1 \rightarrow S_0$ transition probed at 550 nm. Since the relative extinction coefficients of FMN in the excited singlet and triplet states are unknown absolute triplet quantum yields cannot be given. However, a global analysis of the transient absorption measurements shows that the quantum yield for triplet formation Φ_{ISC} of LOV2-

Table 1
Fluorescence lifetime τ, radiative lifetime τ_{RAD}, quantum yields Φ for fluorescence (FL), internal conversion (IC) and triplet formation (ISC) and rates k for IC and ISC of LOV2-WT, LOV2-C39A and FMN free in solution

	τ (ns)	Φ_{FL}	τ_{RAD} (ns)	Φ_{IC}	k_{IC} (ns^{-1})	Φ_{ISC}	k_{ISC} (ns^{-1})
LOV2-WT	2.2	0.14	16.4	0.03	67.1	0.83	2,7
LOV2-C39A	4.3	0.26	17.0	0.07	67.1	0.68	6.5
FMN	4.6	0.26	18.1	0.09	52.2	0.65	7.2

WT is by a factor of 1.23 ± 0.07 higher as compared to the mutant LOV2-C39A. This increase may be due to the combined effects of electrostatics related to the cysteine's polar –SH group and to spin orbit coupling increased by the sulfur atom. The role of electrostatics is underlined by the observation that in comparison to the alanine mutant C39A intersystem crossing is favoured in the respective serine mutant [8]. With respect to the well known high ISC rate in sulfur containing compounds it should be added that the cysteinyl-adduct which is stable at low temperatures does not show fluorescence under steady-state conditions. The residual weak fluorescence observed at 80 K is due to a minority of unbleached FMN in LOV2-WT (data not shown).

Because of the similarity of the steady-state spectra with their pronounced vibronic structure it can be assumed, that in WT and mutant the FMN chromophore is immobilized in the protein binding pocket in a similar way. Assuming that motional freedom of the chromophore correlates with the internal conversion rate, it is probable that these rates are similar. In the following we put this assumption to test by comparing its consequences on the background of the absolute triplet yield $\Phi_{ISC} = 0.88$ [8], which has been independently determined.

The resulting data set for LOV2-WT, LOV2-C39A and FMN in solution is given in Table 1. All rates and quantum yields rest on the assumption $k_{IC}(WT) = k_{IC}(C39A)$, and the experimental data of this paper: fluorescence quantum yields, lifetimes and $\Phi_{ISC}(WT)/\Phi_{ISC}(C39A) = 1.23 \pm 0.07$. This enhancement corresponds to an increase of the ISC rate in LOV2-WT by a factor of 2.4 leading to an absolute quantum efficiency of triplet formation in LOV2-WT of 0.83 ± 0.05 in agreement with the literature [8].

While the increased ISC rate is still consistent with the recent results of Kennis et al. [13], the measurements represented in this paper provide clear evidence that the most important primary reaction in the LOV2 domain is intersystem crossing and that this process leads to a substantial increase of the triplet yield in LOV2-WT as compared to the mutant. This result is in contrast to Ref. [13] where no increase in the triplet yield is reported. Instead the main effect of the protein environment in LOV2-WT as compared to FMN free in solution is an increase of IC rate in the protein by a factor of 5. This discrepancy may be either be related to the different calibration systems, flavin in solution and mutant C39A, or even to differences in the protein preparation.

In contrast to FMN in the C39A mutant and FMN free in solution the increase of the ISC rate and of the respective triplet yield are the most relevant characteristics of the primary photophysics of the wild type LOV2 domain. The triplet states thus formed trigger the formation of the cysteine-adduct which is the key photoproduct responsible for the sensoric function of the LOV2 protein. The general validity of these primary photophysics is also borne out by the comparative ps time-resolved fluorescence study on the LOV1 domain, WT and mutant C57S [26].

Acknowledgements

We are grateful for stimulating discussions with Stephen Weber (FU Berlin) and Gerald Richter (TU München). Financial support from Deutsche Forschungsgemeinschaft (Sonderforschungsbereich 533 and Ru108/31-4) is gratefully acknowledged.

References

[1] W.R. Briggs, E. Huala, Annu. Rev. Cell. Dev. 15 (1999) 33.
[2] C. Fankhauser, J. Chory, Curr. Biol. 9 (1999) R123.
[3] A.R. Cashmore, J.A. Jarillo, Y.-J. Wu, D. Liu, Science 284 (1999) 760.
[4] A. Sancar, Annu. Rev. Biochem. 69 (2000) 31.
[5] E. Huala, P.W. Oeller, E. Liscum, I.-S. Han, E. Larsen, W.R. Briggs, Science 278 (1997) 2120.
[6] M. Salomon, J. Christie, E. Knieb, U. Lempert, W.R. Briggs, Biochemistry 39 (2000) 9401.
[7] S.M. Miller, V. Massey, D. Ballou, C.H. Williams, M.D. Distefano, M.J. Moore, C.T. Walsh, Biochemistry 29 (1990) 2831.
[8] T.E. Swartz, S.B. Corchnoy, J.M. Christie, J.W. Lewis, I. Szundi, W.R. Briggs, R.A. Bogomolni, J. Biol. Chem. 276 (2001) 36493.
[9] S. Crosson, K. Moffat, Proc. Natl. Acad. Sci. USA 98 (2001) 2995.
[10] M. Salomon, W. Eisenreich, H. Dürr, E. Schleicher, E. Knieb, V. Massey, W. Rüdiger, F. Müller, A. Bacher, G. Richter, Proc. Natl. Acad. Sci. USA 98 (2001) 12357.
[11] S. Crosson, K. Moffat, The Plant Cell 14 (2002) 1067.
[12] T.E. Swartz, P. Wenzel, S. Corchnoy, W.R. Briggs, R. Bogomolni, Biochemistry 41 (2002) 7183.
[13] J.T. Kennis, S. Crosson, M. Gauden, I.H. van Stokkum, K. Moffat, R. van Grondelle, Biochemistry 42 (2003) 3385.
[14] M.E. Michel-Beyerle, H. Scheer, H. Seidlitz, D. Tempus, R. Haberkorn, FEBS Lett. 100 (1979) 9.
[15] M. Volk, A. Ogrodnik, M.E. Michel-Beyerle, in: R.E. Blankenship, M.T. Madigan, C.E. Bauer (Eds.), Anoxygenic Photosynthetic Bacteria, Kluwer Academic Publishers, Dordrecht, 1999, p. 595.
[16] D. Zhong, A.H. Zewail, Proc. Natl. Acad. Sci. USA 98 (2001) 11867.
[17] S. Weber, C.W.M. Kay, H. Mögling, K. Möbius, K. Hitomi, T. Todo, Proc. Natl. Acad. Sci. USA 99 (2002) 1319.
[18] C.W. Kay, E. Schleicher, A. Kuppig, H. Hofner, W. Rüdiger, M. Schleicher, M. Fischer, A. Bacher, S. Weber, G. Richter, J. Biol. Chem. 278 (2003) 10973.
[19] J.M. Christie, M. Salomon, K. Nozue, M. Wada, W.R. Briggs, Proc. Natl. Acad. Sci. USA 96 (1999) 8779.
[20] D. Magde, R. Wong, P.G. Seybold, Photochem. Photobiol. 75 (2002) 327.
[21] H. Lossau, A. Kummer, R. Heinecke, F. Pöllinger-Dammer, C. Kompa, G. Bieser, T. Jonsson, C.M. Silva, M.M. Yang, D.C. Youvan, M.E. Michel-Beyerle, Chem. Phys. 213 (1996) 1.
[22] F. Pöllinger, C. Musewald, H. Heitele, M.E. Michel-Beyerle, C. Anders, M. Futscher, G. Voit, H. Staab, Ber. Bunsenges. Phys. Chem. 100 (1996) 2076.
[23] P.F. Heelis, Chem. Soc. Rev. 11 (1982) 15.
[24] F. Müller, S.G. Meyhew, V. Massey, Biochemistry 12 (1973) 4654.
[25] J.K. Eweg, F. Müller, A.J. Visser, C. Veeger, D. Bebelaar, J.D. van Voorst, Photochem. Photobiol. 30 (1979) 463.
[26] W. Holzer, A. Penzkofer, M. Fuhrmann, P. Hegemann, Photochem. Photobiol. 75 (2002) 479.
[27] S. Gishla, Methods Enzymol. 66 (1980) 360.
[28] F. Müller, Free Flavins: Syntheses, Chemical and Physical Properties in Chemistry and Biochemistry of Flavoenzymes, CRC Press, Boca Raton, 1991.
[29] R. Traber, E. Vogelmann, S. Schreiner, T. Werner, H.E.A. Kramer, Photochem. Photobiol. 33 (1981) 41.
[30] R.W. Chambers, D.R. Kearns, Photochem. Photobiol. 10 (1969) 215.
[31] P.F. Heelis, in: F. Müller (Ed.), Chemistry and biochemistry of flavoenzymes, vol. 1, CRC Press, Boca Raton, 1991, p. 171.
[32] M. Sakai, H. Takahashi, J. Mol. Struct. 379 (1996) 9.
[33] P.F. Heelis, G.O. Phillips, J. Phys. Chem. 89 (1985) 770.